

Fundamental Relations as the Leading Order in Nonlinear Thermoelectric Responses with Time-Reversal Symmetry

Ying-Fei Zhang^{1,*}, Zhi-Fan Zhang^{2,*}, Hua Jiang^{2,3,†}, Zhen-Gang Zhu^{1,4,‡} and Gang Su^{5,6§}

¹*School of Physical Sciences, University of Chinese Academy of Sciences, Beijing 100049, China.*

²*Interdisciplinary Center for Theoretical Physics and Information Sciences, Fudan University, Shanghai 200433, China.*

³*State Key Laboratory of Surface Physics, Fudan University, Shanghai 200433, China.*

⁴*School of Electronic, Electrical and Communication Engineering,*

University of Chinese Academy of Sciences, Beijing 100049, China.

⁵*Kavli Institute for Theoretical Sciences, University of Chinese Academy of Sciences, Beijing 100190, China.*

⁶*Institute of Theoretical Physics, Chinese Academy of Sciences, Beijing 100190, China.*

In recent years, nonlinear transport phenomena have garnered significant interest in both theoretical explorations and experiments. In this work, we utilize the semi-classical wave packet theory to calculate disorder-induced second-order transport coefficients: second-order electrical (σ), thermoelectric (α), and thermal (κ) coefficients, capturing the interplay between side-jump and skew-scattering contributions in systems with time-reversal symmetry. Using a topological insulator model, we quantitatively characterize the Fermi-level dependence of these second-order transport coefficients by explicitly including Coulomb impurity potentials. Furthermore, we elucidate the relationships between these coefficients, establishing the second-order Mott relation and the Wiedemann-Franz law induced by disorder. This study develops a comprehensive theoretical framework elucidating the nonlinear thermoelectric transport mechanisms in quantum material systems.

Thermoelectric transport plays an important role in condensed matter physics, such as the anomalous Hall effect and Nernst effect [1–6]. Based on the linear response theory, the Mott relation and Wiedemann-Franz (WF) law have been observed and proved [2, 7–9], which reveals general relations between charge currents or heat currents driven by an electric field or temperature gradient in systems with broken time-reversal symmetry (TRS). Unfortunately, these relationships no longer hold in systems with TRS because the linear Hall effect vanishes as the integrated Berry curvature equals zero [10–12].

However, striking progress has been made recently: a nonlinear response may be induced in TRS materials with broken inversion symmetry (\mathcal{P} -broken) [13]. Importantly the nonlinear responses are dominant as leading order since the linear responses may disappear in some cases. Moreover, the nonlinear responses for charge, spin, and heat are deeply rooted in the intrinsic properties of systems, for example, the Berry curvature dipole (BCD) [13–16]. The BCD reveals that particular pattern of distribution of Berry curvature in momentum space and brings us observable effects [17–22]. For a comparison, the linear Hall effect (the intrinsic mechanism for anomalous Hall effect or quantum Hall effect [23–26]) is an integral of Berry curvature over the entire momentum space. In some sense, nonlinear responses provide a powerful tool to study more detailed properties of systems.

These phenomena can be traced back to the second-order nonlinear Hall effect [13, 16, 27–37], the second-order thermoelectric effect [38–49], and the second-order thermal effect [6, 47, 50, 51], whose response currents are proportional to the square of the driving electric field or temperature gradient. Three contributions can be identified for these effects: intrinsic (in), and two ex-

trinsic terms, namely side-jump (sj) and skew-scattering (sk).

Identifying the mutual relationships between different dynamical quantities is a fundamental issue and may reveal deep insights into the microscopic physics of systems. Recent progress in nonlinear transport has shown a deep and subtle interplay between charge, spin, heat, and topological properties of Bloch bands. In the second-order nonlinear regime induced by BCD, the anomalous Hall and Nernst coefficients are proposed to be directly proportional to each other, $\sigma \propto \alpha$ [14, 15], and the anomalous thermal Hall coefficient satisfies $\kappa \propto \frac{\partial \sigma}{\partial \mu}$ [15] or $\sigma \propto \frac{\partial \kappa}{\partial \mu}$ [14]. Thus, we are confronted with a key question: what are the correct fundamental relations in the nonlinear regime? Furthermore, if disorder is inevitably present, how these relationships are modified by impurity scattering? As far as we know, the influence of impurities on nonlinear thermoelectric effects is non-negligible.

In this work, we perform a comprehensive analysis of the impact of impurity scattering on the second-order thermoelectric effect using the semi-classical method (Table I). Using the surface states of topological insulators (TIs), we show that skew scattering (sk) makes a dominant contribution to the second-order Hall effect where the BCD is zero due to C_{3v} symmetry. Meanwhile, we find the relationships among all the coefficients when considering Coulomb screening scattering (Table II). Intriguingly, for side-jump (sj) scattering, the relation among the three second-order thermoelectric response coefficients ($\alpha_{xxy}^{sj} = -\frac{L}{3}\sigma_{xxy}^{sj}$ and $\frac{\partial \kappa_{xxy}^{sj}}{\partial \varepsilon_F} = \frac{L}{3e}\sigma_{xxy}^{sj}$) is independent of the scattering potential and model details. As for sk scattering, we obtain the relations $\alpha_{xxy}^{sk} = LP\sigma_{xxy}^{sk}$ and $\frac{\partial \kappa_{xxy}^{sk}}{\partial \varepsilon_F} = -\frac{L}{e}P\sigma_{xxy}^{sk}$, where P is a parameter related

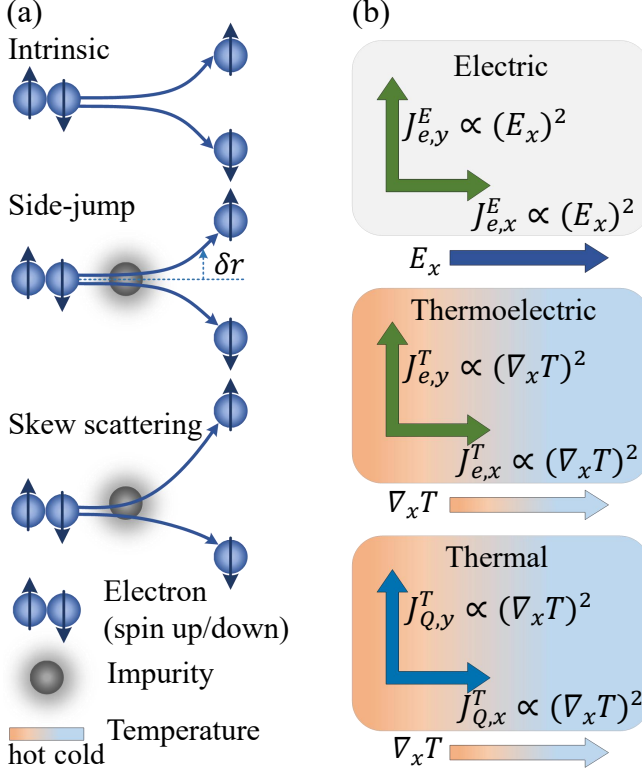


FIG. 1. (a) Illustration of the intrinsic and two other extrinsic mechanisms that can give rise to nonlinear response. (b) Diagrams of transverse and longitudinal electric, thermal and thermoelectric effects, where the electric field or temperature gradient is along the direction of x .

to the Coulomb potential.

For TRS systems driven by an electric field \mathbf{E} or temperature gradient $\nabla\mathbf{T}$, we can write the charge current \mathbf{J}_e and heat current \mathbf{J}_Q in component form as [12, 52–56]

$$\begin{aligned} J_{e,a} &= J_{e,a}^E + J_{e,a}^T = \sigma_{abc} E_b E_c + \alpha_{abc} (-\nabla_b T) (-\nabla_c T), \\ J_{Q,a} &= J_{Q,a}^E + J_{Q,a}^T = \tilde{\alpha}_{abc} E_b E_c + \kappa_{abc} (-\nabla_b T) (-\nabla_c T), \end{aligned} \quad (1)$$

where $a, b, c \in \{x, y, z\}$ denote the Cartesian indices, with the Einstein summation convention implied for repeated indices (b, c) . $J_{e,a}^{E(T)}$ represents the a -th component of response electric currents driving by \mathbf{E} ($\nabla\mathbf{T}$), and $J_{Q,a}^{E(T)}$ corresponds to the a -th component of response heat currents driving by \mathbf{E} ($\nabla\mathbf{T}$). σ_{abc} , α_{abc} , $\tilde{\alpha}_{abc}$, and κ_{abc} are the second-order electric, thermoelectric, electric-thermal and thermal coefficients, respectively. It should be noted that Eq. (1) does not take into account the mixed second-order terms of driving electric field and temperature gradient [57–60], which we will consider in future work.

In order to better describe the response effects of real materials, we consider three major contributions to the response, as illustrated in Fig. 1 [28, 41, 45, 50]. After some steps of derivation (see [61] for more details),

Table I shows the organized form of the three transport coefficients expressed as [28, 41]

$$C_{m_1, m_2}^{\text{in/sj/sk}} = - \int d\varepsilon \mathcal{X}_{m_1}^{\text{in/sj/sk}} \left(\frac{\varepsilon - \mu}{k_B T} \right)^{m_2} \frac{\partial f_0}{\partial \varepsilon}, \quad (2)$$

where $m_1 \in \{1, 2, 3, 4, 5\}$ and $m_2 \in \{0, 1, 2, 3\}$, ε represents energy, k_B represents the Boltzmann constant, T is temperature, and f_0 is the Fermi-Dirac equilibrium distribution of electrons in absence of external electric field or temperature gradient.

Unlike linear responses [28, 45], the kernel functions in the second-order nonlinear response derived in this work possess distinct forms. The first one is an intrinsic contribution induced by BCD (we name it as intrinsic since this term is induced by the anomalous velocity due to Berry curvature of Bloch bands)

$$\mathcal{X}_1^{\text{in}} = \tau \frac{\epsilon_{abd}}{\hbar} \int_k \Omega_{k_d} v_{k_c}^g \frac{\partial f_0}{\partial \varepsilon_k}, \quad (3)$$

where τ is the relaxation time, ϵ_{abd} is the Levi-Civita symbol and $a, b, c, d \in \{x, y, z\}$, \hbar is the Planck constant, $\int_k = \int \frac{d^D k}{(2\pi)^D}$ with the dimension D , $v_{k_c}^g = \frac{1}{\hbar} \frac{\partial \varepsilon_k}{\partial k_c}$ is the group velocity, ε_k is the energy marked by the wave vector k , and Berry curvature Ω_k , a gauge-field tensor, is crucial in all Hall-like effects. It is clearly visible that this second-order response is proportional to τ . In time-reversal symmetric systems, numerous experiments investigating the second-order response have been conducted in recent years, drawing significant attention [17–22].

The side-jump scattering from the side-jump velocity and the anomalous distribution is the second mechanism we consider. And the kernel functions are

$$\mathcal{X}_1^{\text{sj}} = \tau^2 \int_k v_{k_a}^{\text{sj}} v_{k_b}^g v_{k_c}^g \frac{\partial^2 f_0}{\partial \varepsilon_k^2}, \quad (4a)$$

$$\mathcal{X}_2^{\text{sj}} = \tau^2 \int_k \left(v_{k_a}^{\text{sj}} \Gamma_{bc} + v_{k_b}^{\text{sj}} \Gamma_{ac} \right) \frac{\partial f_0}{\partial \varepsilon_k}, \quad (4b)$$

$$\mathcal{X}_3^{\text{sj}} = \tau^2 \int_k v_{k_a}^g \int_{k'} w_{kk'}^{(S)} v_{k'_c}^g \delta r_{b,k'k} \frac{\partial^2 f_0}{\partial \varepsilon_k^2}, \quad (4c)$$

$$\mathcal{X}_{p=4,5}^{\text{sj}} = \tau^2 \frac{2}{p-3} \int_k (2v_{k_a}^g v_{k_b}^{\text{sj}} - v_{k_a}^{\text{sj}} v_{k_b}^g) v_{k_c}^g \frac{\partial^{p-3} f_0}{\partial \varepsilon_k^{p-3}}, \quad (4d)$$

where $\Gamma_{ij} = \frac{\partial v_{k_i}^g}{\hbar \partial k_j} = \frac{\partial^2 \varepsilon_k}{\hbar^2 \partial k_i \partial k_j}$ is the Hessian matrix [62], inversely proportional to the effective mass of the electron. Under the approximation of large effective mass, the contribution of this term can be neglected ($\Gamma_{ij} \rightarrow 0$). $w_{kk'}^{(S)}$ is the symmetric scattering rate. Overall, the sj scattering is all proportional to $\tau^2 v_k^{\text{sj}} \propto \tau$, with $v_k^{\text{sj}} = \int_{k'} w_{kk'}^{(S)} \delta r_{k'k} \propto \tau^{-1}$ and $\delta r_{k'k}$ the coordinate shift [63, 64], indicating that we might need additional scaling to distinguish sj from that of intrinsic contribution. For electric field driving, the sj term is rather complex

TABLE I. The anomalous transport coefficients with TRS. 2nd means the second-order.

2nd nonlinear effect	intrinsic	skew scattering	side-jump
Electric	$\sigma_{abc}^{in} = -e^3 C_{1,0}^{in}$ [13]	$\sigma_{abc}^{sk} = e^3 (C_{1,0}^{sk} - C_{2,0}^{sk})$	$\sigma_{abc}^{sj} = -e^3 (C_{1,0}^{sj} + C_{2,0}^{sj} - C_{3,0}^{sj})$
Thermoelectric	$\alpha_{abc}^{in} = -ek_B^2 C_{1,2}^{in}$ [14, 15]	$\alpha_{abc}^{sk} = -ek_B^2 \left(\frac{1}{k_B T} C_{3,1}^{sk} + C_{4,2}^{sk} \right)$	$\alpha_{abc}^{sj} = ek_B^2 \left(\frac{1}{k_B T} C_{4,1}^{sj} + C_{5,2}^{sj} \right)$
Thermal	$\kappa_{abc}^{in} = -k_B^3 T C_{1,3}^{in}$ [14]	$\kappa_{abc}^{sk} = k_B^2 (C_{3,2}^{sk} + k_B T C_{4,3}^{sk})$	$\kappa_{abc}^{sj} = -k_B^2 (C_{4,2}^{sj} + k_B T C_{5,3}^{sj})$

and can be decomposed into three parts [Eqs. (4a)-(4c)]. Apart from the term [Eq. (4b)] relating to the effective mass, the other two terms [Eqs. (4a) and (4c)] can be approximately regarded as the contributions of \mathbf{v}_k^{sj} and the square of \mathbf{v}_k^g , which indicates that they are highly related to the shape of the energy band in the k -space. However, as for the driving of the temperature gradient, the effective mass of electrons does not directly affect the second-order thermoelectric or thermal effects based on the Eq. (4d).

Lastly, the sk scattering, which are asymmetric scattering due to the effective spin-orbit coupling of the electron or impurity, reads

$$\mathcal{X}_1^{sk} = \tau^3 \int_k \int_{k'} \left(\Gamma_{ac} v_{k'_b}^g + v_{k'_a}^g \Gamma_{bc} \right) w_{kk'}^{(A)} \frac{\partial f_0}{\partial \varepsilon_k}, \quad (5a)$$

$$\mathcal{X}_2^{sk} = \tau^3 \int_k \int_{k'} v_{k_a}^g v_{k'_b}^g v_{k'_c}^g w_{kk'}^{(A)} \frac{\partial^2 f_0}{\partial \varepsilon_k^2}, \quad (5b)$$

$$\mathcal{X}_{q=3,4}^{sk} = \tau^3 \frac{4}{q-2} \int_k \int_{k'} v_{k_a}^g v_{k_b}^g v_{k_c}^g w_{kk'}^{(A)} \frac{\partial^{q-2} f_0}{\partial \varepsilon_k^{q-2}}, \quad (5c)$$

where $w_{k'/k}^{(A)}$ is the anti-symmetric scattering rate from k to k' . Without loss of generality, we consider the third order skew scattering which is $w_{k'/k}^{(A)} \propto \tau^0$. It is seen that the contribution from sk scattering is proportional to τ^3 [Eqs. (5a)-(5c)]. Since the longitudinal linear conductivity is proportional to τ , the sk scattering [Eqs. (5a)-(5c)] can in principle be distinguished from the intrinsic [Eq. (3)] and side-jump terms [Eqs. (4a)-(4d)] (they are both proportional to τ) through the scaling relation to the longitudinal linear conductivity.

We take the surface state of TI X_2Y_3 ($X=Bi$, $Y=Se$, Te) as an example, with its crystal structure shown in Fig. 2(a) [65, 66]. It is evident that the structure exhibits C_{3v} symmetry and the corresponding Hamiltonian is

$$H(k) = v(k_x \sigma_y - k_y \sigma_x) + \frac{\lambda}{2} (k_+^3 + k_-^3) \sigma_z, \quad (6)$$

where v is the Dirac velocity, $k_{\pm} = k_x \pm ik_y = ke^{i\theta_k}$, $\sigma_{x,y,z}$ are the Pauli matrixes, and the parameter λ serves as a quantitative descriptor for the magnitude of hexagonal warping in the electronic structure. The energy dispersion is $\varepsilon_{\pm,k} = \pm \sqrt{k^2 v^2 + k^6 \lambda^2 \cos^2(3\theta_k)}$. In addition, the Berry curvature linearly in the warping strength λ is $\Omega_{k_z} \approx \frac{\lambda}{v} \cos(3\theta_k) + O(\lambda^2)$.

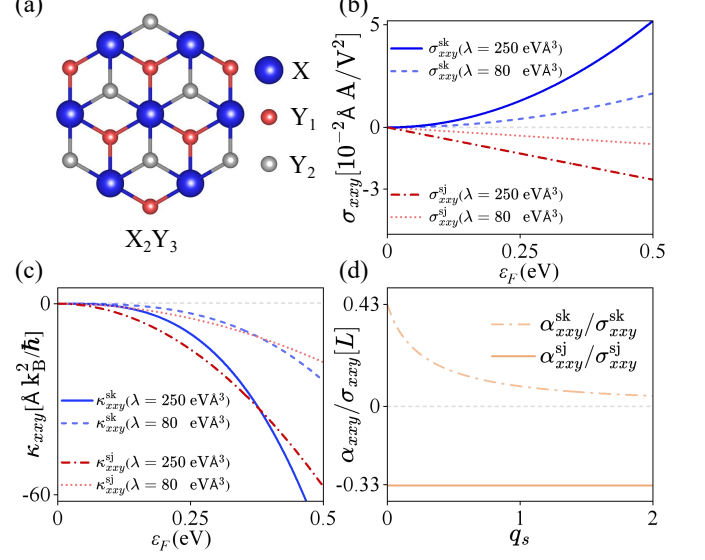


FIG. 2. (a) Crystal structure of the surface of the topological insulator X_2Y_3 . The hexagonal lattice is projected along the (001) direction. (b) Variation of the second-order Hall coefficient $\sigma_{xxy}^{sk/sj}$ with Fermi energy ε_F under different λ . (c) Fermi energy ε_F dependence of the second-order thermal coefficient $\kappa_{xxy}^{sk/sj}$ for different λ . (d) Calculated ratio $\alpha_{xxy}^{sk/sj}/\sigma_{xxy}^{sk/sj}$ in unit of L as a function of q_s . The gray dot line in (b)-(d) is shown for visual guidance. Parameters used: $v = 3.291 \text{ eV}\text{\AA}$, $\lambda = 80 \text{ eV}\text{\AA}^3, 250 \text{ eV}\text{\AA}^3$, $\tau = 0.1 \text{ ps}$.

In principle, we need to distinguish whether the nonlinear current originates from the Berry curvature dipole, quantum metric, or extrinsic contributions (sj, sk, or other mixing terms), based on criteria such as crystal symmetry, scaling law, or other means. Nonetheless, within the framework of our model, it should be noted that the τ -independent contribution arising from quantum metric [67–69] is strictly forbidden due to the \mathcal{P} -broken but with TRS. Meanwhile, due to the C_{3v} symmetry, the second-order intrinsic effect induced by the BCD vanishes and only the two extrinsic contributions from impurity scattering exists [13, 27]. To be specific, the independent nonzero elements are only those of the $\sigma_{xxy} = \sigma_{xyx} = \sigma_{yx} = -\sigma_{yyy}$ [27].

For the present Hamiltonian, the absence of momentum dependence in a δ -correlated random potential re-

TABLE II. The second-order (2nd) Mott relation and Wiedemann-Franz (WF) Law induced by disorder, where P is a dimensionless quantity determined by the strength of Coulomb interaction q_s [61], and $L = \frac{\pi^2 k_B^2}{3e^2}$ is the Lorentz number.

	side-jump	skew scattering
2nd Mott	$\alpha_{xxy}^{sj} = -\frac{1}{3}L\sigma_{xxy}^{sj}$	$\alpha_{xxy}^{sk} = LP\sigma_{xxy}^{sk}$
2nd WF law	$\frac{\partial\kappa_{xxy}^{sj}}{\partial\varepsilon_F} = \frac{L}{3e}\sigma_{xxy}^{sj}$	$\frac{\partial\kappa_{xxy}^{sk}}{\partial\varepsilon_F} = -\frac{L}{e}P\sigma_{xxy}^{sk}$

sults in the vanishing of $w_{k'k}^{(A)}$, implying that such impurities make no skew scattering contribution to the second-order response [36]. This issue can be circumvented by considering the screened Coulomb impurities [36, 37, 70, 71] that are randomly dispersed within the sample. Beginning with the bare Coulomb potential in real space, $V_0(r) = \frac{e^2 Q}{4\pi\varepsilon_0\varepsilon r}$ captures the interaction between charge carriers and a charge impurity Q , where r is the carrier-impurity separation and $\varepsilon_0(\varepsilon)$ is the vacuum (material) permittivity. Through Fourier transformation and considering Thomas-Fermi screening at long wavelength, the screened Coulomb interaction takes the form $V(q) = \frac{2\pi\alpha v}{q+q_{TF}}$, where $q = |\mathbf{k} - \mathbf{k}'|$ is the magnitude of the momentum transfer for an electron scattered from an initial state \mathbf{k} to a final state \mathbf{k}' , α is a dimensionless coupling constant analogous to the fine-structure constant [70], q_{TF} represents the Thomas-Fermi wave vector, and we define $q_s = \frac{q_{TF}}{k_F}$. Experimentally, the ratio $\frac{q_{TF}}{k_F}$ requires three key physical quantities, the carrier density, Fermi velocity, and effective dielectric constant, which can be extracted from Hall bar transport measurements, scanning tunnelling microscopy and angle-resolved photoemission spectroscopy(such as $\frac{q_{TF}}{k_F} \lesssim 0.4$ for Bi_2Se_3 [70]). The scattering rate and relaxation time are both closely related to q_s , which indicate that the magnitude of Coulomb interaction is crucial to the second-order thermometric transport.

It can be shown in this model that a nonzero warping term is essential for generating a finite second-order response due to disorder, i.e. $\lambda \neq 0$. Following a laborious calculation, we derive the second-order electric, thermoelectric and thermal response coefficients for the xxy component (more details in [61]). In Fig. 2(b), the skew scattering and side-jump contributions of the second-order electric response coefficients scale as $\sigma_{xxy}^{sk} \propto \varepsilon_F^4$ and $\sigma_{xxy}^{sj} \propto \varepsilon_F^2$, respectively. These scaling behaviors indicate that tuning the chemical potential away from the band edge significantly enhances the second-order response, in agreement with experimental observations [70]. Notably, the two contributions display opposite signs, wherein the skew scattering term plays a dominant role compared to the side-jump component. However, for the second-order thermal response, there are different scaling be-

haviors. $\kappa_{xxy}^{sk} \propto \varepsilon_F^5$ and $\kappa_{xxy}^{sj} \propto \varepsilon_F^3$, the skew scattering term grows more rapidly with increasing ε_F . As seen in Fig. 2(c), at higher Fermi energies, the thermal response becomes increasingly dominated by the skew scattering mechanism, which is significantly larger than the side-jump scattering contribution. Besides, to highlight the role of hexagonal warping in the second-order disorder-induced response, we consider two representative values of the warping parameter $\lambda = 80$ and $250 \text{ eV}\text{\AA}^3$ shown in Figs. 2(b) and (c), which correspond to two topological insulators Bi_2Se_3 [65, 70] and Bi_2Te_3 [66], respectively. It is evident that an increase in the wrapping term results in a corresponding augmentation of the second-order response coefficients.

Furthermore, when considering the Coulomb impurities, we obtain the second-order Mott relation, $\alpha_{xxy}^{sj} = -\frac{1}{3}L\sigma_{xxy}^{sj}$ and $\alpha_{xxy}^{sk} = LP\sigma_{xxy}^{sk}$, and the second-order WF law, $\frac{\partial\kappa_{xxy}^{sj}}{\partial\varepsilon_F} = \frac{L}{3e}\sigma_{xxy}^{sj}$ and $\frac{\partial\kappa_{xxy}^{sk}}{\partial\varepsilon_F} = -\frac{L}{e}P\sigma_{xxy}^{sk}$ (Table II), where P is just a function of parameter q_s . Overall, the coefficients that describe these relationships can be classified into two categories based on the contribution of impurities. The skew scattering exhibits a diminishing trend with increasing the Coulomb interaction's strength q_s ; while the side-jump contribution yields a constant ratio that is independent of q_s . Specially for the second-order Mott relation, we simply show this trend in Fig. 2(d). In the limit of $q_s \rightarrow 0$, we still have fundamental relations that don't depend on the details of the model ($\alpha_{xxy}^{sk} \approx 0.43L\sigma_{xxy}^{sk}$). Similarly, the second-order WF law of the sk term can be expressed as $\frac{\partial\kappa_{xxy}^{sk}}{\partial\varepsilon_F} \approx -0.43\frac{L}{e}\sigma_{xxy}^{sk}$ when q_s approaches zero [61].

Although we try our best to obtain the general relationship of the second-order thermoelectric coefficients, there are still some points that we don't take into consideration. We only take into account the contribution of the highest-order relaxation time for sj and sk scattering. We note that there are other contributions related to the interband Berry connection that has no counterpart in linear response [72–74], which may also affect the relations. In addition, we would like to point out that there are some other methods in the research field of topological nonlinear transport, such as Feynman diagrams [14, 27, 75–77], density matrices [46, 78–80] or nonequilibrium Green's function formalism [81–83]. Moreover, we only consider the case of TRS in this work, we expect that under other symmetries, such as \mathcal{PT} symmetry [29, 30, 47, 59], these relations will also get certain modifications due to the contributions of quantum metric dipole. Simultaneously, the impact of electron-electron correlation [84–87] effects on the self-energy and vertex corrections, as well as their subsequent modifications to the thermoelectric transport responses and fundamental relations, which are not considered in our current study, remain an area that warrants further investigation.

Finally, we would like to point out that the Mott re-

lation induced by sk scattering in our theoretical work is qualitatively consistent with the recent experimental observation [48], where the proportionality between the second-order Nernst conductivity and the Hall conductivity due to the skew scattering is verified (see Extended Data Fig. 4 in Ref. [48]). Crucially, beyond merely capturing the sk-induced Mott-like trends, our study establishes microscopic theoretical basis within semiclassical framework, as detailed in Table I. More importantly, aside from the experimentally verified sk-Mott term, we provide the first theoretical predictions for the remaining three fundamental relations in Table II. The results in our work establish a comprehensive theoretical foundation that accounts for the disorder-induced transport mechanisms.

This work is supported by the National Key R&D Program of China (Grant No. 2024YFA1409200, No. 2022YFA1402802, and No. 2022YFA1403700), CAS Project for Young Scientists in Basic Research Grant No. YSBR-057, and the NSFC (Grant No. 12350401). G.S. is supported in part by the Innovation Program for Quantum Science and Technology (Grant No. 2024ZD0300500), NSFC (Grant No. 12447101), and the Strategic Priority Research Program of Chinese Academy of Sciences (Grant No. XDB1270000).

* These authors contributed equally to this work.

† jianghuaphy@fudan.edu.cn

‡ zgzhuc@ucas.ac.cn

§ gstu@ucas.ac.cn

- [1] N. Nagaosa, J. Sinova, S. Onoda, A. H. MacDonald, and N. P. Ong, Anomalous Hall effect, *Rev. Modern Phys.* **82**, 1539 (2010).
- [2] D. Xiao, Y. Yao, Z. Fang, and Q. Niu, Berry-phase effect in anomalous thermoelectric transport, *Phys. Rev. Lett.* **97**, 026603 (2006).
- [3] D. L. Bergman and V. Oganesyan, Theory of dissipationless Nernst effects, *Phys. Rev. Lett.* **104**, 066601 (2010).
- [4] C. Zhang, S. Tewari, V. M. Yakovenko, and S. Das Sarma, Anomalous Nernst effect from a chiral-density-wave state in underdoped cuprate superconductors, *Phys. Rev. B* **78**, 174508 (2008).
- [5] C. Zhang, S. Tewari, and S. Das Sarma, Berry-phase-mediated topological thermoelectric transport in gapped single and bilayer graphene, *Phys. Rev. B* **79**, 245424 (2009).
- [6] L. Zhang, Berry curvature and various thermal Hall effects, *New J. Phys.* **18**, 103039 (2016).
- [7] M. Jonson and G. D. Mahan, Mott's formula for the thermopower and the Wiedemann-Franz law, *Phys. Rev. B* **21**, 4223 (1980).
- [8] T. Yokoyama and S. Murakami, Transverse magnetic heat transport on the surface of a topological insulator, *Phys. Rev. B* **83**, 161407 (2011).
- [9] N. M. Neil Ashcroft, Solid state physics (Brooks Cole; New edition (2 Jan. 1976), 1976).
- [10] D. Xiao, M.-C. Chang, and Q. Niu, Berry phase effects

- on electronic properties, *Rev. Modern Phys.* **82**, 1959 (2010).
- [11] K. Behnia and H. Aubin, Nernst effect in metals and superconductors: a review of concepts and experiments, *Rep. Prog. Phys.* **79**, 046502 (2016).
- [12] C. Ortix, Nonlinear Hall effect with time-reversal symmetry: Theory and material realizations, *Adv. Quantum Technol.* **4**, 2100056 (2021).
- [13] I. Sodemann and L. Fu, Quantum Nonlinear Hall Effect Induced by Berry Curvature Dipole in Time-Reversal Invariant Materials, *Phys. Rev. Lett.* **115**, 216806 (2015).
- [14] Y. Wang, Z.-G. Zhu, and G. Su, Quantum theory of nonlinear thermal response, *Phys. Rev. B* **106**, 035148 (2022).
- [15] C. Zeng, S. Nandy, and S. Tewari, Fundamental relations for anomalous thermoelectric transport coefficients in the nonlinear regime, *Phys. Rev. Research* **2**, 032066 (2020).
- [16] Z.-F. Zhang, Z.-G. Zhu, and G. Su, Intrinsic second-order spin current, *Phys. Rev. B* **110**, 174434 (2024).
- [17] S. Duan, F. Qin, P. Chen, X. Yang, C. Qiu, J. Huang, G. Liu, Z. Li, X. Bi, F. Meng, X. Xi, J. Yao, T. Ideue, B. Lian, Y. Iwasa, and H. Yuan, Berry curvature dipole generation and helicity-to-spin conversion at symmetry-mismatched heterointerfaces, *Nat. Nanotechnol.* **18**, 867 (2023).
- [18] S.-Y. Xu, Q. Ma, H. Shen, V. Fatemi, S. Wu, T.-R. Chang, G. Chang, A. M. M. Valdivia, C.-K. Chan, Q. D. Gibson, J. Zhou, Z. Liu, K. Watanabe, T. Taniguchi, H. Lin, R. J. Cava, L. Fu, N. Gedik, and P. Jarillo-Herrero, Electrically switchable Berry curvature dipole in the monolayer topological insulator WTe₂, *Nat. Phys.* **14**, 900 (2018).
- [19] Q. Ma, S.-Y. Xu, H. Shen, D. MacNeill, V. Fatemi, T.-R. Chang, A. M. M. Valdivia, S. Wu, Z. Du, C.-H. Hsu, S. Fang, Q. D. Gibson, K. Watanabe, T. Taniguchi, R. J. Cava, E. Kaxiras, H.-Z. Lu, H. Lin, L. Fu, N. Gedik, and P. Jarillo-Herrero, Observation of the nonlinear Hall effect under time-reversal-symmetric conditions, *Nature* **565**, 337 (2018).
- [20] K. Kang, T. Li, E. Sohn, J. Shan, and K. F. Mak, Nonlinear anomalous Hall effect in few-layer WTe₂, *Nat. Mater.* **18**, 324 (2019).
- [21] J. Xiao, Y. Wang, H. Wang, C. D. Pemmaraju, S. Wang, P. Muscher, E. J. Sie, C. M. Nyby, T. P. Devoreaux, X. Qian, X. Zhang, and A. M. Lindenberg, Berry curvature memory through electrically driven stacking transitions, *Nat. Phys.* **16**, 1028 (2020).
- [22] R.-C. Xiao, D.-F. Shao, Z.-Q. Zhang, and H. Jiang, Two-dimensional metals for piezoelectriclike devices based on Berry-curvature dipole, *Phys. Rev. Applied* **13**, 044014 (2020).
- [23] S.-Q. Shen, Topological insulators: Dirac equation in condensed matter, *Springer Ser. Solid-State Sci.* **0171-1873**, **187**, 266 (2017).
- [24] K. v. Klitzing, G. Dorda, and M. Pepper, New method for high-accuracy determination of the fine-structure constant based on quantized Hall resistance, *Phys. Rev. Lett.* **45**, 494 (1980).
- [25] D. J. Thouless, M. Kohmoto, M. P. Nightingale, and M. den Nijs, Quantized Hall conductance in a two-dimensional periodic potential, *Phys. Rev. Lett.* **49**, 405 (1982).
- [26] F. D. M. Haldane, Model for a quantum Hall effect without Landau levels: Condensed-matter realization of the

“parity anomaly”, *Phys. Rev. Lett.* **61**, 2015 (1988).

[27] Z. Z. Du, C. M. Wang, H. -P. Sun, H. -Z. Lu, and X. C. Xie, Quantum theory of the nonlinear Hall effect, *Nat. Commun.* **12**, 5038 (2021).

[28] Z. Z. Du, C. M. Wang, S. Li, H.-Z. Lu, and X. C. Xie, Disorder-induced nonlinear Hall effect with time-reversal symmetry, *Nat. Commun.* **10**, 3047 (2019).

[29] C. Wang, Y. Gao, and D. Xiao, Intrinsic nonlinear Hall effect in antiferromagnetic tetragonal CuMnAs, *Phys. Rev. Lett.* **127**, 277201 (2021).

[30] H. Liu, J. Zhao, Y.-X. Huang, W. Wu, X.-L. Sheng, C. Xiao, and S. A. Yang, Intrinsic second-order anomalous Hall effect and its application in compensated anti-ferromagnets, *Phys. Rev. Lett.* **127**, 277202 (2021).

[31] J. Duan, Y. Jian, Y. Gao, H. Peng, J. Zhong, Q. Feng, J. Mao, and Y. Yao, Giant second-order nonlinear Hall effect in twisted bilayer graphene, *Phys. Rev. Lett.* **129**, 186801 (2022).

[32] K. Das, S. Lahiri, R. B. Atencia, D. Culcer, and A. Agarwal, Intrinsic nonlinear conductivities induced by the quantum metric, *Phys. Rev. B* **108**, 1201405 (2023).

[33] J. M. Adhidewata, R. W. M. Komalig, M. S. Ukhtary, A. R. T. Nugraha, B. E. Gunara, and E. H. Hasdeo, Trigonal warping effects on optical properties of anomalous Hall materials, *Phys. Rev. B* **107**, 155415 (2023).

[34] S. Saha and A. Narayan, Nonlinear Hall effect in Rashba systems with hexagonal warping, *J. Phys. Condens. Matter* **35**, 485301 (2023).

[35] Y. Wang, Z. Zhang, Z.-G. Zhu, and G. Su, Intrinsic nonlinear Ohmic current, *Phys. Rev. B* **109**, 085419 (2024).

[36] H. Isobe, S.-Y. Xu, and L. Fu, High-frequency rectification via chiral Bloch electrons, *Sci. Adv.* **6**, eaay2497 (2020).

[37] P. Makushko, S. Kovalev, Y. Zabila, I. Ilyakov, A. Ponomaryov, A. Arshad, G. L. Prajapati, T. V. A. G. de Oliveira, J.-C. Deinert, P. Chekhonin, I. Veremchuk, T. Kosub, Y. Skourski, F. Ganss, D. Makarov, and C. Ortix, A tunable room-temperature nonlinear Hall effect in elemental bismuth thin films, *Nat. Electron.* **7**, 207 (2024).

[38] Y. Gao and D. Xiao, Orbital magnetic quadrupole moment and nonlinear anomalous thermoelectric transport, *Phys. Rev. B* **98**, 060402 (2018).

[39] C. Zeng, S. Nandy, A. Taraphder, and S. Tewari, Nonlinear Nernst effect in bilayer WTe₂, *Phys. Rev. B* **100**, 245102 (2019).

[40] X.-Q. Yu, Z.-G. Zhu, and G. Su, Hexagonal warping induced nonlinear planar Nernst effect in nonmagnetic topological insulators, *Phys. Rev. B* **103**, 035410 (2021).

[41] M. Papaj and L. Fu, Enhanced anomalous Nernst effect in disordered Dirac and Weyl materials, *Phys. Rev. B* **103**, 075424 (2021).

[42] C. Zeng, S. Nandy, and S. Tewari, Nonlinear transport in Weyl semimetals induced by Berry curvature dipole, *Phys. Rev. B* **103**, 245119 (2021).

[43] C. Zeng, S. Nandy, and S. Tewari, Chiral anomaly induced nonlinear Nernst and thermal Hall effects in Weyl semimetals, *Phys. Rev. B* **105**, 125131 (2022).

[44] C. Zeng, X.-Q. Yu, Z.-M. Yu, and Y. Yao, Band tilt induced nonlinear Nernst effect in topological insulators: An efficient generation of high-performance spin polarization, *Phys. Rev. B* **106**, 1081121 (2022).

[45] X.-B. Qiang, Z. Z. Du, H.-Z. Lu, and X. C. Xie, Topological and disorder corrections to the transverse Wiedemann-Franz law and Mott relation in kagome magnets and Dirac materials, *Phys. Rev. B* **107**, 161302 (2023).

[46] H. Varshney and A. Agarwal, Intrinsic nonlinear Nernst and Seebeck effect, *New J. Phys.* **27**, 083506 (2025).

[47] Y.-F. Zhang, Z.-F. Zhang, Z.-G. Zhu, and G. Su, Second-order intrinsic Wiedemann-Franz law, *Phys. Rev. B* **111**, 165424 (2025).

[48] H. Liu, J. Li, Z. Zhang, *et al.*, Nonlinear Nernst effect in trilayer graphene at zero magnetic field, *Nat. Nanotech.* **20**, 1221–1227 (2025).

[49] X.-Q. Yu, Z.-G. Zhu, J.-S. You, T. Low, G. Su, Topological nonlinear anomalous Nernst effect in strained transition metal dichalcogenides, *Phys. Rev. B* **99**, 201410 (2019).

[50] D.-K. Zhou, Z.-F. Zhang, X.-Q. Yu, Z.-G. Zhu, and G. Su, Fundamental distinction between intrinsic and extrinsic nonlinear thermal Hall effects, *Phys. Rev. B* **105**, 1201103 (2022).

[51] J.-C. Li and Z.-G. Zhu, Intrinsic second-order magnon thermal Hall effect, *J. Phys. Condens. Matter* **36**, 395802 (2024).

[52] M. Itskov, *Tensor Algebra and Tensor Analysis for Engineers: With Applications to Continuum Mechanics*, Springer, Cham (2025).

[53] C. Li, *Nonlinear Optics: Principles and Applications*, Springer, Singapore (2017).

[54] Z. Z. Du, H.-Z. Lu, and X. C. Xie, Nonlinear Hall effects, *Nat. Rev. Phys.* **3**, 744–752 (2021).

[55] N.-X. Yang, Q. Yan, and Q.-F. Sun, Linear and nonlinear thermoelectric transport in a magnetic topological insulator nanoribbon with a domain wall, *Phys. Rev. B* **102**, 245412 (2020).

[56] T. A. Costi and V. Zlatić, Thermoelectric transport through strongly correlated quantum dots, *Phys. Rev. B* **81**, 235127 (2010).

[57] R. Nakai and N. Nagaosa, Nonreciprocal thermal and thermoelectric transport of electrons in noncentrosymmetric crystals, *Phys. Rev. B* **99**, 115201 (2019).

[58] T. Yamaguchi, K. Nakazawa, and A. Yamakage, Microscopic theory of nonlinear Hall effect induced by electric field and temperature gradient, *Phys. Rev. B* **109**, 205117 (2024).

[59] X. Yang and B. Skinner, Nonlinear thermoelectric effects as a means to probe quantum geometry, arXiv (2025), arXiv:2505.00086 [cond-mat.mes-hall].

[60] T. Yamaguchi, K. Nakazawa, and A. Yamakage, Theory of nonlinear Hall effect induced by electric field and temperature gradient in 3D chiral magnetic textures, arXiv (2024), arXiv:2410.00563 [cond-mat.mes-hall].

[61] The supplementary material gives details of methods and results: SI) Derivation of second-order nonlinear thermoelectric effects; SII) The surface state of the topological insulator, which includes refs. [1,2,6,14,16,29,37,38,42,64,66].

[62] Y. Gao, Semiclassical dynamics and nonlinear charge current, *Front Phys.* **14**, 33404 (2019).

[63] N. A. Sinitsyn, Q. Niu, J. Sinova, and K. Nomura, Disorder effects in the anomalous Hall effect induced by Berry curvature, *Phys. Rev. B* **72**, 045346 (2005).

[64] N. A. Sinitsyn, Q. Niu, and A. H. MacDonald, Coordinate shift in the semiclassical Boltzmann equation and the anomalous Hall effect, *Phys. Rev. B* **73**, 075318 (2006).

[65] K. Kuroda, M. Arita, K. Miyamoto, M. Ye, J. Jiang, A. Kimura, E. E. Krasovskii, E. V. Chulkov, H. Iwasawa, T. Okuda, K. Shimada, Y. Ueda, H. Namatame, and M. Taniguchi, Hexagonally deformed fermi surface of the 3D topological insulator Bi_2Se_3 , *Phys. Rev. Lett.* **105**, 076802 (2010).

[66] L. Fu, Hexagonal warping effects in the surface states of the topological insulator Be_2Te_3 , *Phys. Rev. Lett.* **103**, 266801 (2009).

[67] A. Gao, N. Nagaosa, N. Ni, and S.-Y. Xu, Quantum geometry phenomena in condensed matter systems, [arXiv:2508.00469](https://arxiv.org/abs/2508.00469) (2025).

[68] T. Liu, X.-B. Qiang, H.-Z. Lu, and X. C. Xie, Quantum geometry in condensed matter, *Natl. Sci. Rev.* **12**, nwaee334 (2024).

[69] J. Yu, B. A. Bernevig, R. Queiroz, E. Rossi, P. Törmä, and B.-J. Yang, Quantum geometry in quantum materials, *npj Quantum Mater.* **10**, 1 (2025).

[70] P. He, H. Isobe, D. Zhu, C.-H. Hsu, L. Fu, and H. Yang, Quantum frequency doubling in the topological insulator Bi_2Se_3 , *Nat. Commun.* **12**, 689 (2021).

[71] X. F. Lu, C.-P. Zhang, N. Wang, D. Zhao, X. Zhou, W. Gao, X. H. Chen, K. T. Law, and K. P. Loh, Nonlinear transport and radio frequency rectification in BiTeBr at room temperature, *Nat. Commun.* **15**, 1 (2024).

[72] Z.-H. Gong, Z. Z. Du, H.-P. Sun, H.-Z. Lu, and X. C. Xie, Nonlinear transport theory at the order of quantum metric, [arXiv:2410.04995 \[cond-mat.mes-hall\]](https://arxiv.org/abs/2410.04995).

[73] C. Xiao, Z. Z. Du, and Q. Niu, Theory of nonlinear Hall effects: Modified semiclassics from quantum kinetics, *Phys. Rev. B* **100**, 165422 (2019).

[74] M. Mehraeen, Quantum kinetic theory of quadratic responses, *Phys. Rev. B* **110**, 174423 (2024).

[75] N. A. Sinitsyn, A. H. MacDonald, T. Jungwirth, V. K. Dugaev, and J. Sinova, Anomalous hall effect in a two-dimensional dirac band: The link between the Kubo-Streda formula and the semiclassical Boltzmann equation approach, *Phys. Rev. B* **75**, 045315 (2007).

[76] D. E. Parker, T. Morimoto, J. Orenstein, and J. E. Moore, Diagrammatic approach to nonlinear optical response with application to Weyl semimetals, *Phys. Rev. B* **99**, 045121 (2019).

[77] H. Bruus and K. Flensberg, *Many-Body Quantum Theory in Condensed Matter Physics: An Introduction*, edited by online (Oxford University Press, 2004).

[78] P. Bhalla, Intrinsic contribution to nonlinear thermoelectric effects in topological insulators, *Phys. Rev. B* **103**, 115304 (2021).

[79] H. Varshney, K. Das, P. Bhalla, and A. Agarwal, Quantum kinetic theory of nonlinear thermal current, *Phys. Rev. B* **107**, 235419 (2023).

[80] D. Ma, Z. F. Zhang, H. Jiang, and X. C. Xie, Quantum kinetic theory of the semiclassical side jump, skew scattering, and longitudinal velocity, *Phys. Rev. B* **112**, 045136 (2025).

[81] M. Wei, B. Wang, Y. Yu, F. Xu, and J. Wang, Nonlinear Hall effect induced by internal Coulomb interaction and phase relaxation process in a four-terminal system with time-reversal symmetry, *Phys. Rev. B* **105**, 115411 (2022).

[82] L. Zhang, F. Xu, J. Chen, Y. Xing, and J. Wang, Quantum nonlinear ac transport theory at low frequency, *New J. Phys.* **25**, 113006 (2023).

[83] G. Li, M. Wei, F. Xu, and J. Wang, General method for calculating transport properties of disordered mesoscopic systems based on the nonequilibrium Green's function formalism, *Phys. Rev. B* **111**, 035409 (2025).

[84] I. Pasqua and M. Fabrizio, Fermi-liquid corrections to the intrinsic anomalous Hall conductivity of topological metals, *SciPost Phys.* **19**, 014 (2025).

[85] Y.-S. Jho, J.-H. Han, and K.-S. Kim, Topological fermi-liquid theory for interacting weyl metals with time reversal symmetry breaking, *Phys. Rev. B* **95**, 205113 (2017).

[86] J.-Y. Chen and D. T. Son, Berry fermi liquid theory, *Ann. Phys-new. York.* **377**, 345 (2017).

[87] M. Wang, J. Zhou, and Y. Yao, Linear and nonlinear optical responses in Green's function formula, [arXiv:2508.07280](https://arxiv.org/abs/2508.07280) (2025).

.